Published in final edited form as:
Cell Stem Cell. 2009 February 6; 4(2): 155–169. doi:10.1016/j.stem.2008.12.009.

A Two-Step Mechanism for Stem Cell Activation during Hair Regeneration

Valentina Greco[1,3], **Ting Chen**[1,3], **Michael Rendl**[1,2], **Markus Schober**[1], **H. Amalia Pasolli**[1], **Nicole Stokes**[1], **June dela Cruz-Racelis**[1], and **Elaine Fuchs**[1,*]

[1] Howard Hughes Medical Institute, The Rockefeller University, New York, NY 10065, USA

SUMMARY

Hair follicles (HFs) undergo cyclic bouts of degeneration, rest, and regeneration. During rest (telogen), the hair germ (HG) appears as a small cell cluster between the slow-cycling bulge and dermal papilla (DP). Here we show that HG cells are derived from bulge stem cells (SCs) but become responsive quicker to DP-promoting signals. In vitro, HG cells also proliferate sooner but display shorter-lived potential than bulge cells. Molecularly, they more closely resemble activated bulge rather than transit-amplifying (matrix) cells. Transcriptional profiling reveals precocious activity of both HG and DP in late telogen, accompanied by Wnt signaling in HG and elevated FGFs and BMP inhibitors in DP. FGFs and BMP inhibitors participate with Wnts in exerting selective and potent stimuli to the HG both in vivo and in vitro. Our findings suggest a model where HG cells fuel initial steps in hair regeneration, while the bulge is the engine maintaining the process.

INTRODUCTION

Adult stem cells (SCs) function in tissue homeostasis and wound repair. They are often characterized by their slowly cycling nature and their location within a niche, features thought to preserve their ability to self-renew and remain undifferentiated over the lifetime of the animal (Schofield, 1978). In the adult skin, slow-cycling, relatively undifferentiated SCs exist within a niche known as the bulge, located below the sebaceous gland in the outer root sheath (ORS) of the hair follicle (HF) (Cotsarelis et al., 1990; Oshima et al., 2001; Taylor et al., 2000). Recently, it was shown that slow-cycling bulge cells form during embryonic skin development (Nowak et al., 2008). Both in neonatal and adult mice, bulge cells are typified by certain key SC markers including Sox9, Lhx2, NFATc1, Tcf3, and Lgr5 (Merrill et al., 2001; Tumbar et al., 2004; Morris et al., 2004; Blanpain et al., 2004; Rhee et al., 2006; Vidal et al., 2005; Nguyen et al., 2006; Horsley et al., 2008; Nowak et al., 2008; Jaks et al., 2008). Specified during embryogenesis, nascent HFs respond to underlying mesenchymal condensates (DP progenitors) and grow downward until they mature and begin to produce hair (Schmidt-Ull-rich and Paus, 2005). Completion of HF morphogenesis requires input from Sox9-positive bulge cells, which appear to fuel production of transiently amplifying (TA), highly proliferative (matrix) cells that envelope the DP at the follicle base (Nowak et al., 2008). Although not unequivocal, the outermost layer of the lower ORS is thought to contain migrating cells that move from the bulge toward the matrix (Oshima et al., 2001).

[*]Correspondence: fuchslb@rockefeller.edu.
[2]Present address: Black Family Stem Cell Institute, Department of Developmental and Regenerative Biology, Mount Sinai School of Medicine, New York, NY 10029, USA
[3]These authors contributed equally to this work

Following this first growth phase (anagen), backskin HFs enter an apoptotic destructive phase known as catagen. During catagen, the HF is reduced to a thin epithelial strand surrounded by a basement membrane. As it retracts, the DP is pulled upward to the base of the permanent portion of the HF where SCs in the bulge reside. The ensuing resting phase (telogen) lasts 1 to 2 days before the new hair growth emerges. With this transition from telogen to anagen, the HF begins a new cycle, a process that continues throughout life. Although the lengths of anagen and catagen phases are similar from one cycle to the next, each telogen becomes progressively longer than the previous one. During the second telogen, the DP and the epithelial portion of the HF are in contact for nearly 4 weeks, and the third telogen is even longer. These increasingly prolonged telogen phases result in progressive asynchrony in HF cycling with age (Muller-Rover et al., 2001).

Two signaling pathways are known to participate in driving HFs from telogen to anagen. Central to this process is the stabilization of β-catenin, an established effector of active Wnt signaling and a transcriptional cofactor for Lef1/Tcf proteins (Gat et al., 1998; Lo Celso et al., 2004; Lowry et al., 2005; Van Mater et al., 2003; Zhang et al., 2008). Equally important is epithelial-mesenchymal crosstalk, which in part involves bone morphogenetic protein (BMP) signaling. Active BMP signaling is critical for the DP (Rendl et al., 2008) and for maintaining bulge SCs in a relatively quiescent state (Blanpain et al., 2004; Horsley et al., 2008). Inhibition of BMP signaling induces morphogenesis and cycling (Botchkarev et al., 2001; Kobielak et al., 2007). Recently, it was discovered that waves of BMP expression in the dermis occur out of phase with the Wnt/β-catenin cycle, thereby subdividing telogen into a (high BMP) refractory phase and a (low BMP) competent phase for hair regeneration (Plikus et al., 2008).

A number of questions remain in understanding how SCs become activated at the start of a new hair cycle. Why is transition between permissive and repressive states for hair growth so abrupt after sometimes lengthy states of dormancy? How does the follicle avoid depleting all its SCs during the transition to growth? Are there pathways in addition to Wnt signaling and BMP inhibition that are involved in regulating this transition?

To begin to address these questions, we monitored the extended second telogen phase of the hair cycle and dissected the earliest steps involved in SC activation and HF regeneration. We focused on two subcompartments of the lower follicle that exist throughout this resting period: the CD34(+), slow-cycling bulge cells and the (secondary) hair germ (HG or germ), a small cluster of P-cadherin-enriched cells that forms at the end of catagen and separates bulge from underlying DP (Lyle et al., 1999; Muller-Rover et al., 1999; Panteleyev et al., 2001). The origin of the HG has been a matter of speculation. The lateral disc hypothesis proposes that the bulge and HG represent distinct populations of SCs maintained in separate niches at all stages of the hair cycle. In this scenario, the HG is equivalent to the small pocket of Shh-expressing cells in the matrix at the base of the anagen phase HF (Panteleyev et al., 2001). An alternative view is that the HG derives from CD34(+), label-retaining cells (LRCs) in the bulge. This could happen either directly at the transition from catagen to telogen, as proposed by Ito et al. (2004), or indirectly from surviving stem cells that exited the bulge but were not utilized before catagen was initiated (Panteleyev et al., 2001).

In this report, we show that the HG maintains its size, shape, and morphology throughout telogen, where it persists as an ultrastructurally distinct entity. Our genetic lineage tracing shows that while Shh-expressing cells generate inner root sheath (IRS), they do not survive catagen and hence do not represent the HG. Rather, although our studies do not distinguish between direct and indirect mechanisms, our BrdU pulse-chase studies support the bulge as the precursor of the HG. We further show that toward the end of telogen, the HG stabilizes β-catenin and initiates mitogen-activated phosphokinase (MAPK) signaling. We uncover a

two-step activation process: HG cells proliferate several days before bulge cells and are the major contributors to the first stage in HF regeneration. In vitro, HG cells also initiate colonies more rapidly than bulge cells but display reduced long-term growth potential relative to bulge cells.

Finally, we have purified and transcriptionally profiled bulge, HG, and DP populations at early, mid-, and late telogen. We found that during the resting phase, both HG and DP are transcriptionally more dynamic than bulge cells and that key signaling proteins required for the telogen to anagen transition accumulate in these compartments in late telogen. Unexpectedly, FGF7 and, to a lesser extent, FGF10 progressively increase in expression within the DP during telogen. Using a combination of in vitro and in vivo strategies, we demonstrate that FGF signaling contributes to the telogen to anagen transition, adding new insights into the process of stem cell activation.

RESULTS

The HG Forms at the Catagen-to-Telogen Transition but Does Not Originate from the Shh-Expressing Lateral Disc

To investigate the relation between bulge and HG, we monitored SCs as HFs transit from catagen through the extended second telogen and into the next cycle (Figure 1A; Muller-Rover et al., 2001). During this time, both CD34(+) bulge and P-cadherin-enriched ($Pcad^{Hi}$) HG populations were faithfully maintained (Figure 1B). Additionally, $Pcad^{Hi}$ cells remained relatively constant in number, suggesting that this compartment is largely quiescent during telogen (Figure 1C). This was further substantiated by H2BGFP pulse-chase experiments (Tumbar et al., 2004), where overall label retention patterns were largely unchanged over telogen and a few LRCs resided in the $Pcad^{Hi}$ HG compartment (Figure 1D).

Ultrastructural analyses revealed distinct morphological differences between bulge and HG compartments (Figure S1). Most notably, HG cells displayed fewer desmosomes than bulge cells. This was true even when bulge and HG cells in direct contact with the basement membrane were compared. Given these distinctions, we revisited the hypotheses regarding HG origins.

We first tested the lateral disc hypothesis by employing genetic lineage tracing with *$ShhCre^{ER}$/Rosa-LoxP-Stop-LoxP-LacZ* mice. If the hypothesis is correct, then *Shh*-Cre activation in the disc at the end of anagen should lead to βgal(+) cells in the HG. In late anagen, βgal(+) progeny of the disc were traced to IRS and HS cuticle (Figure 1E). In telogen, however, both bulge and HG were negative, and the few remaining βgal(+) cells localized to the club hairs (Figure 1E).

When HFs were labeled with BrdU for 2 days in late anagen and then chased, matrix diluted out label by 4 days, restricting slow-cycling LRCs to bulge and ORS (Figure 1F). By 6 days, LRCs were still detected in epithelial strand and bulge, while at 9 days, bulge and HG were labeled. Like the HG, the epithelial strand was positive for both P-cadherin (Figure 1G) and Sox9 (Figure S3A). A few cells within the strand were morphologically similar to the HG, marked by a paucity of desmosomes (Figure S2). Finally, anti-Ki67 immunofluorescence (Figure 1G) and shorter nucleotide pulse-chase experiments (data not shown) revealed that the bulge was largely dormant during catagen and telogen. These data support the notion that whether direct or indirect, the germ is derived from the bulge.

The Hair Germ Contributes to the Next Hair Cycle

We next monitored proliferation from telogen onset to the new anagen by pulsing animals with BrdU for 1 day prior to harvesting (Figures 2A and 2B; Figure S3B). During early and

midtelogen, the HG incorporated little or no label consistent with our label retaining data. At P69, when the bulge was still quiescent and overall HG cell numbers remained constant, ~40% of HGs showed BrdU incorporation. Late telogen phase HGs also contained a significantly higher percentage of G2/M phase cells (3.6%) than either the CD34(+) GFP(+) bulge (0.5%) or the total K14-GFP^{+} population (2%) (Figure 2C). By contrast, it was only well into anagen when LRCs marked in telogen appeared as a trail from the bulge (Figure 2D). By P70, HGs exhibited ≥1 BrdU(+) cell, and by P75, virtually all HGs were positive (Figure S3B). Analogous results were observed with Ki67 (data not shown). Moreover, the bulk of BrdU/Ki67(+) cells were also Pcad^{Hi} and CD34(−), further demonstrating that CD34(+) bulge cells remain relatively quiescent into early anagen.

Similar results were obtained for the first postnatal hair cycle. Thus, in late telogen (P21), Pcad^{Hi} HGs became Ki67/BrdU(+) (Figures 2E–2J). Moreover, by BrdU lineage tracing, we observed that as HFs initiated new growth (P22-P23), HGs expanded and the intensity of their BrdU labeling waned. In contrast, the bulge remained silent at this time and did not show activity until several days later, when proliferation became obvious starting at anagen II (Figures 1A and 2K; Figure S3C). Thus, even though most bulge cells cycle ~3× during each hair cycle (Waghmare et al., 2008), the HG is the principal source of the rapidly proliferating cells that contribute to the initial transition into anagen. This agrees well with hair-plucking experiments showing that bulge LRCs are delayed in division relative to HG cells (Morris and Potten, 1999; see also Panteleyev et al., 2001).

Hair Germ Cells Form Large Colonies More Quickly than CD34(+) Bulge Cells But Their Long Term Potential is Poorer In Vitro

To better understand the relation between HG and CD34(+) bulge cells, we used FACS to purify cells from P69 late telogen mice expressing H2BGFP driven by the *keratin 14* (*K14)* promoter. An epithelial gene was essential, as other markers such as CD34 are expressed broadly in the dermis. As control, we used total H2BGFP(+) cells (Figure 3A). Primary keratinocytes (1°MK) were then plated at low clonal density (Blanpain et al., 2004) and monitored by their H2BGFP epifluorescence.

Within hours, GFP(+) cells from Bulge and HG adhered equivalently (Figure 3B). After only 3 days, GFP(+)Pcad^{Hi}CD34(−) HG cultures displayed ~17× more colonies (defined as ≥4 cells) than GFP(+)Pcad^{lo}CD34(+) bulge cultures (Figure 3C). Of the cells that initially attached after plating (Figure 3B), ~50% of HG but only 5% of bulge cells progressed by 5 days to form colonies with an average size of 17–32 cells (Figure 3D). Differences in colony numbers were corroborated by total MK numbers quantified by FACS (Figure 3E and Figure S4B).

Some initially attached single cells later detached either through death or differentiation (Figure S4A). However, both HG and bulge formed large (≥20 mm^2) colonies of >1000 tightly packed cells (Figures 3F and 3G and Figure S4C), resembling the so-called holoclones that are purported to be the consequences of SC culture (Barrandon and Green, 1987). Interestingly, HG cells generated large colonies much more rapidly than bulge cells, but by 10 days, both bulge and all GFP populations continued to generate large colonies, and differences between HG and bulge colony number dwindled to ~4× (Figure 3C). Since in vivo the bulge is larger than the HG, the total in vitro output of large colonies with characteristics of holoclones was comparable for these two compartments (Figure 3G).

Stemness necessitates the ability not only to form compact large colonies but also to withstand long-term passaging (Barrandon and Green, 1987). When large colonies were randomly picked and passaged, bulge cells consistently generated more large colonies and survived for >9 passages (Figure 3H; Blanpain et al., 2004). By contrast, HG cells typically

failed to grow beyond passage 3 to 4, even when cells were pooled and passaged to optimizechances of revealing SC characteristics (data not shown).

Similar to our experience with cultures from FACS-purified adult epidermis/upper ORS (Blanpain et al., 2004), the inability to passage HG cells long term precluded engraftment as a mean to test lineage capacity. Moreover, since existing promoters (*K15* and *Lgr5*) for lineage tracing do not distinguish between bulge and HG (Morris et al., 2004; Jaks et al., 2008), evaluating the relative in vivo potency of bulge versus HG cells is presently not possible. That said, the ability of HG cells to repopulate the bulge when depleted of its SCs (Ito et al., 2004) is consistent with our finding that even though HG cells failed the test for long-term stemness in vitro, they still have considerable proliferative potential.

The Hair Germ: Molecularly Distinct from Bulge, ORS, and Matrix

To probe more deeply into the characteristics of HG cells, we next examined classical markers for bulge, ORS, and transit-amplifying (TA) matrix (Figures 4A–4C). Of the six bulge markers tested, CD34 and NFATc1 were absent and Sox9 was diminished in the HG. The germ also differed from matrix. Thus, while anti-Lef1 labeled both HG and matrix, HGs showed no expression of *Shh*, *Wnt10b*, and *Msx2* (Figures 4A–4C; data not shown). These patterns were suggestive of a transitional state, unique from both bulge and matrix. Further evidence to this point is provided below.

Previous studies indicate that at the start of the hair cycle, the emerging nascent HF displays nuclear β-catenin, typical of Wnt-signaling (Lo Celso et al., 2004; Lowry et al., 2005; Merrill et al., 2001; Van Mater et al., 2003). Interestingly, toward the end of telogen, β-catenin stabilization occurred concomitant with Ki67 in the HG (Figure 4D). Although interactions with the DP are thought to stimulate β-catenin stabilization in HF SCs, weeks of continual contact between DP and HG preceded this event.

To explore this relation further, we used a genetic model in which postnatal de novo HF morphogenesis is initiated atypically as a consequence of an N-terminally truncated, stabilized form of β-catenin (Gat et al., 1998). At the onset of ectopic HF initiation, β-catenin-induced outgrowths were positive for Ki67 and P-cadherin, but not CD34 (Figure 4E). These data suggest that P-cadherin, nuclear β-catenin, and Ki67 are features of cells initiating HFs. Notably, these are also features of embryonic HGs, recently shown to be composed of short-lived cells that are replaced by Sox9(+) early bulge cells during HF morphogenesis (Nowak et al., 2008; Rhee et al., 2006).

Hair Germ Cells Are Transcriptionally More Active than Telogen-Phase Bulge Cells

To better understand what drives the selective change in proliferative status of the HG toward the end of telogen, we transcriptionally profiled the HG and bulge at early, mid-, and late telogen, i.e., times when their morphology was unchanged (Figure S5). HG and bulge mRNAs shared many probe sets called as present in two independent array data sets (Figure 5A). This was expected, since many of them correspond to housekeeping and/or proliferation-associated genes. That said, ~20% of probe sets were differentially expressed in the two populations.

By using a functional gene annotation tool (DAVID 2008), probe sets were subdivided into categories. By comparing expression trends of genes within categories, we learned that during telogen, the HG is transcriptionally more dynamic than bulge (Figure 5B). Additionally, whole microarray comparisons consistently revealed a broader range of HG versus bulge changes (Figure 5C, left histogram). This spread was particularly conspicuous when comparisons were made that included late telogen profiles, underscoring the precocious activation of HG at this time (Figure 5C, right histogram).

Molecular Relation between Hair Germ and Activated Bulge SCs

We next created molecular signatures composed of proteins whose transcripts are up- or downregulated by ≥2× in either bulge or HG relative to the other at equivalent telogen stages. Real time PCR, in situ hybridizations, and immunofluorescence microscopy validated these signatures and highlighted molecular differences between the two compartments (Figure 5D; see also Figure 4). Consistent with and extending our immunofluorescence data, genes encoding many key HF SC markers were either absent (NFATc1, CD34, and S100A6) or markedly diminished (Lgr5 and Sox9) in HG (Figures 5D and 5E). Analogously, while the bulge signature was enriched for genes encoding cell-cycle arrest, Wnt inhibitory, and TGFβ accessory proteins, the P69 HG signature included genes encoding Wnts and MAPK signaling proteins as well as proteins involved in cell-cycle progression. Thus, at a time preceding mitoses, the P69 HG, but not the bulge, showed early signs of enhanced proliferative and signaling activity at the transcriptional level.

The elevation in Wnt gene expression within P69 HGs was intriguing in light of their associated stabilization of β-catenin and the known role for Wnt signaling in transitioning from telogen to anagen (Lo Celso et al., 2004; Lowry et al., 2005; Van Mater et al., 2003). Further insights into the significance of these findings were obtained by comparing signatures of our P69 WT HG and midtelogen bulge purified from *K14*-ΔN*βcat* mice expressing a constitutively stabilized β-catenin (Gat et al., 1998; Lowry et al., 2005). Interestingly, 10 of the 14 bulge genes most strongly upregulated upon β-catenin stabilization (Lowry et al., 2005) were also strongly upregulated in WT HGs compared to the bulge (the encoded proteins are bolded in red in Figure 5E).

Another notable similarity was found between the WT HG as it progressed from early to late telogen (Figure 5E) and the WT bulge as it transitioned from telogen into anagen (Lowry et al., 2005). Shared signature genes included those encoding cell-cycle regulatory proteins, Egr2, Sox4, and Sox7. Together, these findings suggest that an effect resembling Wnt signaling occurs first in the HG (in late telogen) and then later in bulge (in anagen), with the consequence of sequentially stimulating these two compartments to drive the hair cycle.

Finally, we compared our adult late telogen HG signature with signatures of embryonic hair placode/HG, adult telogen versus anagen bulge and matrix, all contrasted against basal cells of epidermis/upper ORS (see the Supplemental Experimental Procedures) (Lowry et al., 2005; Rendl et al., 2005; Rhee et al., 2006). Although cross-comparisons of different data sets precluded absolute signal comparisons, the data were useful in deriving qualitative trends. Of these comparisons, the activated late telogen HG resembled most closely the full anagen bulge (Figure 5F). Interestingly, when activated bulge was compared to quiescent HG at the beginning of telogen, the overlap with activated bulge was reduced (Figure 5F).

Refining the Bulge Signature: Genes Upregulated in the Bulge When Compared Against Both Epidermal and Hair Lineages

While our previous telogen bulge signature was determined by comparing to basal epidermis/upper ORS cells (Blanpain et al., 2004; Lowry et al., 2005; Tumbar et al., 2004), our new signature was derived by comparing to HG. ~50% of encoded proteins upregulated ≥2× were common to both bulge signatures. Included in the telogen bulge signature after refinement against two skin lineages were Bmp6, FGF18, and NFATc1, involved in SC quiescence; essential SC transcription factors Lhx2, Sox9, and Tcf3; and key SC markers Lgr5, CD34, and S100A6 (Table S1).

Dermal Papilla Cells Are Also Transcriptionally Dynamic during Telogen

DP is an essential stimulus for the hair cycle and directly contacts the HG. To explore its possible role in HG stimulation, we used *K14H2BGFP*/*Lef1RFP* mice (Rendl et al., 2005) and simultaneously purified and transcriptionally profiled DP, bulge, and HG at early, mid-, and late telogen (Figures S6 and S7). We derived a molecular signature of genes >3× up-/downregulated in P69 DP relative to P43 DP and used bioinformatics to classify them. In so doing, we discovered that like the HG, the DP is also transcriptionally dynamic during telogen (Figures 6A and 6B).

Particularly notable was the progressively enhanced transcription of genes within the "extracellular signal" category, which contains transcripts encoding putative hair-cycle-stimulating factors (Figure 6B). Further analyses revealed that 26 of these DP genes elevated expression as telogen progressed (Figures 6C–6F). Sostdc1 stood out as a potent inhibitor of BMP signaling, an important pathway in maintaining bulge SCs in a quiescent state (Blanpain et al., 2004; Horsley et al., 2008; Kobielak et al., 2007; Plikus et al., 2008). While several other BMP inhibitors including Bambi displayed a similar trend, BMPs were present throughout telogen. Since the inductive effects of BMP inhibitors are well established, we did not pursue them further here.

FGF7 and, to a lesser extent, its relative FGF10 were also among DP signature genes elevated during telogen (Figures 6C–6E). The timing of FGF7/FGF10 in DP coincided with an increase in MAPK pathway components in the HG (Map4K5, Map3K12; Figure 5E). This was intriguing in light of previous studies, which suggested a paracrine role for FGF7/10 signaling in epidermal wound repair and hair growth (Guo et al., 1996; Suzuki et al., 2000; Werner et al., 1994). By contrast, FGF18 showed higher DP expression at the beginning than end of telogen (shown). The opposing trend for FGF18 was consistent with its growth-inhibitory effects on bulge SCs in vitro (Blanpain et al., 2004).

FGF7 Is a DP Signal that Participates in Instructing HGs to Proliferate and Initiate the New Hair Cycle

To explore the physiological relevance of the increasing trend in FGF7/FGF10 transcription by the DP during telogen, we took advantage of the in vitro colony assay system, which paralleled the in vivo behavior of germ versus bulge. We first screened our growth factors for their effects on the two cell populations. FACS-purified HG and bulge cells were plated at equivalent densities, allowed to attach, and then 2 days later, FGFs (tests) and BMPs (negative controls) were added over a range of concentrations. We measured their effects on the total number of colonies formed within a week after treatment.

FGF7 was particularly effective at stimulating HG cells, doubling the number of colonies overall and increasing their size (Figures 7A and 7B). Bulge cells were more modestly responsive to FGF7. Since both HG and bulge expressed the FGFR2-IIIb receptor specific for FGF7/FGF10 (Figure 7C), the difference in responsiveness appeared to be rooted in the slower cycling activity of bulge cells relative to their HG counterparts (see also Figure 3). Although not positive, the effect of FGF7 on bulge cells was also not inhibitory and in this regard, it differed from the effects of FGF18, whose primary receptor is FGFR3 (Blanpain et al., 2004) (Figure 7A). FGF7's effects also differed from the DP-expressed BMPs, all of which scored as inhibitory for both germ and bulge (shown).

DP's temporal elevation of *FGF7* appeared to be relevant, as it correlated with a temporal rise in both expression and activities of MAPKs in the HG (Figure 7D). To determine whether elevated FGF7 is sufficient to trigger resting HFs to enter a new proliferative phase, we coated beads with 100 ng/μl FGF7 and injected them intradermally into female CD1 mice at P50, when backskin HFs were in early telogen. Within 5 days after bead

implantation, ~85% of P55 HFs adjacent to FGF7-coated beads displayed Ki67(+) HGs, reflective of P69 HFs (Figure 7E). The marked elevation in Ki67 labeling was paralleled by an ~2.5× increase in overall HG size, indicating that midtelogen, HGs had begun to proliferate in response to FGF7 (Figure 7F, upper histogram).

By comparison, very few HGs showed anti-Ki67 immunolabeling if they were not in close vicinity to FGF7 beads or if HFs were instead exposed to either BSA-coated beads (control) or FGF18-coated beads (Figure 7E and middle histogram in Figure 7F). These results were in agreement with our in vitro observations and lent support to the relevance of the opposing DP expression trends of *FGF7* and *FGF18* seen during telogen.

Overall, FGF7's effects were predominantly on HG and not bulge. FGF7 also acted in a dose-dependent fashion, with the highest concentration eliciting the most prominent effect (bottom histogram in Figure 7F). This was also true for FGF10, the closest known relative of FGF7, although the response occurred in fewer HFs and only at the highest dose tested (Figure 7; Figure S8). Thus, although FGF10 was expressed at lower levels in DP and seemed to be somewhat less potent, it may function similarly to FGF7 in skin.

Following HG stimulation, no further expansion or downgrowth was observed. Wnts also appeared to be involved in this early step, as the late telogen HG itself showed elevated signs of Wnt signaling, both transcriptionally (Figure 5E) and by β-catenin stabilization (Figure 4D). In our bead assays BMP inhibitors and WNTs also stimulated P50 telogen HG proliferation, but in addition, they promoted downgrowth (Figure S8; data not shown). Thus, although FGF7 was not sufficient on its own to promote anagen, these data suggest that FGF7 signaling may function in concert with these other pathways to orchestrate new hair growth. Our findings reveal both source and target cells and the time of action for FGF signaling in this process.

DISCUSSION

The Hair Germ: At the Interface of Bulge and Matrix

Our studies unveil the HG as a population of cells morphologically and biologically distinct from the bulge. Like the bulge, these cells are quiescent throughout most of the resting phase of the hair cycle. However, toward the end of telogen, the HG becomes activated, and its constituents are responsible for fueling the first steps of the new hair cycle.

The ability of HG to transition from a quiescent to an activated state resembles the bulge, but its activation occurs earlier, manifesting a two-step process to initiating the hair cycle. The HG's precocious activity during telogen was further reflected by microarray profiling and bioinformatics, which exposed the HG as a more transcriptionally dynamic compartment than the bulge. Notably, many HG signature genes encoding cell-cycle activators and signal transduction pathway members progressively increased their expression throughout telogen. These transcriptional changes coincided with stabilization of β-catenin, activation of MAPK, and induction of proliferation specifically within the HG toward the end of telogen.

During the time when the HG was undergoing marked changes in transcriptional activity, the bulge transcriptional profile remained relatively constant and was enriched for cell-cycle inhibitors and signaling repressors. The bulge was also dormant in proliferative activity during telogen. Intriguingly, however, within several days following the onset of anagen, the bulge seemed to undergo some of these same changes in gene expression and proliferative activity as the HG (Lowry et al., 2005). These transcriptional changes in the anagen bulge also appear to be driven by elevated levels of stabilized β-catenin (Lowry et al., 2005).

These findings underscore the importance of stabilized β-catenin as a hallmark of the transcriptional and proliferative changes occurring in the late telogen HG and early anagen bulge.

Despite these marked resemblances, the late telogen HG displayed a number of differences not detected in anagen bulge. Thus, while certain features of stemness, e.g., Lhx2 and Tcf3, were maintained in HGs, only a small number of HG cells displayed marked label retention, a hallmark of the slow-cycling bulge cells. In addition, many other classical bulge markers scored as either absent (NFATc1, CD34, and S100A6) or diminished transcriptionally and/or biochemically (Lgr5 and Sox9). That said, when compared against the molecular profile of TA matrix cells, the HG much more closely resembled the bulge. Similarly, the ability of HG cells to generate large colonies in vitro with at least some albeit limited passage capacity was clearly distinct from matrix cells that formed few, if any, colonies under these conditions.

What might be the purpose of having two biochemically distinct compartments that both possess some features of stemness and are both involved in the regenerative process? One clue comes from the ability of HG cells to "jump start" colony formation in vitro under conditions where bulge cells were considerably slower to respond. The remarkable ability of HG cells to make large colonies quickly but then exhaust their capacity after a relatively short number of passages was particularly fascinating. Coupled with the increased transcriptional dynamics in these cells, these features suggest that the HG might be endowed with the ability to initiate the burst of cell proliferation necessary to initiate regeneration.

In contrast to the HG, the bulge appeared to be buffered from mobilization during this initial phase. Based upon subsequent bulge activity, it is tempting to speculate that bulge SCs are used more sparingly to extend the ORS and to fuel and maintain the pool of matrix cells, which terminally differentiate after several proliferative cycles. This would explain the ability of bulge cells to undergo slow cycling throughout anagen (Waghmare et al., 2008; J. Nowak and E.F., unpublished data).

While transcriptional and biological changes that lead to bulge cell activation appear to be similar to those within the HG and involve stabilization of β-catenin, it is still unclear why the bulge is delayed in its response. Given that the bulge expresses BMPs (Blanpain et al., 2004), threshold levels of BMP inhibitory cues may be required to tip the balance (Kobielak et al., 2007). The elevation of BMP inhibitory cues within the dermis in the second half of telogen (Plikus et al., 2008) is likely to impact this process, but this should affect both bulge and germ equivalently. It is tempting to speculate that the closer proximity of the HG to the DP makes the difference. The differential transcriptional dynamics support the view that the initial stimulus involves HG-DP interactions, while the subsequent stimuli may emanate from interactions between HG and bulge. What maintains the ability of bulge cells to cycle slowly throughout anagen once the DP has left the niche vicinity awaits future investigation.

Overall, the behavior and biology of the HG suggests that its residents most closely represent activated stem cells. Our findings point to the view that the primary role of the HG is to fuel the initial stages of HF regeneration, in agreement with a model that HG cells are primed and the first responders to DP signals (Panteleyev et al., 2001). By contrast, the bulge appears to be the engine that maintains the growth phase of the hair cycle and houses long-term SCs. The molecular similarities we have uncovered between HG and bulge SCs, coupled with the appreciable proliferative capacity of these cells in vitro, suggest that in contrast to matrix, the HG has not reached a "point of no return" in executing HF terminal differentiation programs. These similarities may also explain why HG cells can nevertheless substitute for SCs when catastrophic bulge vacancies occur (Ito et al., 2004). This notion is

interesting in light of the recent observation that foreign cells can occupy vacancies and adopt SC character when the *Drosophila* female germ SC niche has been emptied (Nystul and Spradling, 2007).

Where Does the Hair Germ Come From and What Is the Long Term Fate of Its Progeny?

While the bulge can be visualized as a biochemically and morphologically defined compartment over the different phases of the hair cycle, the same cannot be said for the HG. The HG is best defined during the quiescent telogen phase where it exists as a stable morphological entity between DP and bulge. Our experiments are consistent with a model where progeny that have exited the bulge could survive until the next cycle and contribute to the HG. Precisely how the HG forms and the fate of its progeny have been difficult to establish, primarily due to the lack of a HG-specific promoter for lineage tracing. Thus, while *K15* (Morris et al., 2004), *Sox9* (Nowak et al., 2008), and *Lgr5* (Jaks et al., 2008) are all active in the HG, they are also expressed in the bulge in telogen and also in the lower ORS (K15, Sox9, *Lgr5*) and matrix (*Lgr5*) and in anagen. Genetic lineage studies with these three promoters complement clonal analyses of cultured CD34(+)/$\alpha6^{hi}$bulge cells (Blanpain et al., 2004) and show that bulge cells after culture or bulge/HG cells within their resident niche(s) in vivo can give rise to all hair lineages. The recent Lgr5 lineage tracing goes one step further in demonstrating that the stem cell potential of Lgr5-marked bulge/HG cells is long term (Jaks et al., 2008). Conversely, our studies here show that the HG becomes activated prior to the bulge at the onset of anagen, and this provides insights into the Jaks study, which measured an increase in S phase cells in LGR5-high (presumably bulge/HG/ORS/matrix) versus CD34-high (presumably bulge/vascular endothelial cell/muscle progenitor) populations within the early anagen phase skin.

Further untangling of the relative contributions of HG versus bulge cells in this process is predicated on the identification of promoters specific to each of these two compartments. In this regard, our array data reveal potential candidates, e.g., *NFATc1* (bulge) and *P-cadherin* (HG). Moreover, in contrast to markers, e.g., CD34, which also expresses dermally, both NFATc1 and P-cadherin are largely restricted to skin epithelium. Such criteria will be essential in developing new and improved tools for future lineage tracing.

While the present set of tools preclude delineation of the precise relation of bulge versus germ, our studies favor the notion that bulge cells give rise to the HG. Lineage analyses will be required to test this hypothesis and further discern whether the HG arises by migration of lower bulge SCs at the end of catagen (Ito et al., 2004) or through preservation of unused cells that may have exited the bulge toward the end of anagen but were left within the epithelial strand during catagen (Panteleyev et al., 2001). In the future, it will be important to distinguish between a model where HF cells can be recycled versus one where commitment is made once an SC has left its niche.

Epithelial-Mesenchymal Crosstalk Regulates Activation of the Hair Germ

The molecular regulation underlying the activation of epithelial HF SCs via signaling by the mesenchymal DP is still poorly understood, even though roles for BMP inhibitors and stabilization of the downstream Wnt effector, β-catenin, are well established. Because SCs stay in close proximity to the DP for an extended resting period prior to embarking upon a new regenerative phase, some additional stimulus must control when SCs become activated. Once we realized that both DP and HG are transcriptionally more dynamic than the bulge, we began to search for a signaling pathway(s) whose key players might progressively increase concomitant with HG activation.

Our search led us to DP signature genes encoding not only BMP antagonists but also FGF7. We showed that transcription of both classes of genes increase markedly as DP transitions from early to late telogen. A role for BMP antagonists in driving the transition to anagen is now well established (Botchkarev et al., 2001; Kobielak et al., 2007; Plikus et al., 2008), and our functional studies with Noggin-soaked beads underscored their importance. However, while loss of FGF7/FGF10 signaling through loss of their specific FGFR2IIIb receptor has long been known to cause defects in the hair coat (Werner et al., 1994; Petiot et al., 2003), our transcriptional and functional studies suggest that FGF7 is a player in the early steps of hair cycle activation. Our studies also indicate that during this initial transition, FGF7 exerts its effects on the HG rather than the bulge, despite the presence of the receptor in both populations. In addition, our studies illuminate the possibility for redundancy between FGF7 and FGF10 in this process.

Our discovery brings together many previous studies that have underscored the importance of the FGF7 signaling in skin (Guo et al., 1996; Werner et al., 1994) but which have failed in unequivocally establishing FGF7's source, its target cells, and the dynamics of its inductive properties during the early steps of hair cycle activation. Moreover, while other FGFs function in the HF, their action occurs during anagen rather than telogen (Hébert et al., 1994). Finally, since genetic alterations in either FGF7 or BMP receptor signaling cause potent mutant hair phenotypes (Botchkarev et al., 2001; Kobielak et al., 2003; 2007; Andl et al., 2004; Plikus et al., 2008; Werner et al., 1994) and since our bead studies support functional roles for both growth factors in stimulating the precocious activation of midtelogen phase HFs, our data point to the view that the two pathways function in concert with Wnt signaling to promote threshold activation of β-catenin stabilization and Wnt target gene expression required for this critical transition. A model summarizing our data is presented in Figure S9.

EXPERIMENTAL PROCEDURES

Mice and Labeling Experiments

pTRE-H2BGFP/K5-tetVP16, *LefRFP*, *K14H2BGFP* and *ShhCre^{ER}/Rosa-LoxP-Stop-LoxP-LacZ* mice were generated previously (Rendl et al., 2005; Tumbar et al., 2004; Levy et al., 2005) and were housed and bred in the CBC ALAAC-accredited animal facility at The Rockefeller University. For H2BGFP pulse-chase experiments, 4-week-old *TRE-H2BGFP/K5Tet^{off}* mice (pulse period) were subsequently fed with doxycycline (Dox) for 4 to 5 weeks (chase period). 5-Bromo-2′-deoxyuridine (BrdU) pulse-chase experiments were performed as described (Blanpain et al., 2004; Alonso et al., 2005). Experiments were performed in duplicate on two different sets of CD-1 littermates of the same sex. For each age/time point, two sets of 50–100 HFs were quantified.

FACS

Cell isolations are described in the Supplemental Experimental Procedures. Cell purifications were performed on a FACSAria system equipped with FACS DiVa software (BD Biosciences). Gates for fluorescence fractionation were set to match those approximated by semiquantitative immunofluorescence analyses of the cell compartments. Cells were first gated for single events and viability and then sorted. For immunofluorescence characterization, cells were FACS-purified and collected with a Cytospin4 unit (Thermo/Shandon). For cell-cycle analyses, FACS-purified cells were incubated at RT for 1 hr with a solution containing propidium iodide (PI), RNase, and Triton X-100. Cell profiling was then performed using an LSR II FACS Analyzer, and analyses were conducted using the FlowJo Program.

Cell Culture

Viability of FACS-isolated keratinocytes was assessed by trypan blue staining, and cell numbers were determined by hemocytometer. Equal numbers of live HG or bulge cells were cultured and expanded as described (Blanpain et al., 2004). After 14 days in vitro, GFP-labeled MKs were trypsinized and counted (Coulter counter; Beckman or FACS LSR II). For factor treatment, cells were plated as described above and on day 2, treated with FGF7 (10 ng/ml), FGF10 (10 ng/ml), FGF18 (10 ng/ml), or Bmp2/4/6/7 (400 ng/ml), as indicated. Colony numbers were determined by counting live cells with GFP epifluorescence.

Supplementary Material

Refer to Web version on PubMed Central for supplementary material.

Acknowledgments

For technical assistance, we thank Andrew Levine (Fuchs Laboratory); Svetlana Mazel, Fan Xiaoxuan, and Chris Bare (Rockefeller FCRD Facility); and Agnes Viale (Genomics Core Facility, MSKI). For suggestions and advice, we thank Mirna Perez-Moreno, Geraldine Guasch, Terry Lechler, and Tudorita Tumbar (Fuchs Laboratory); Sabrina Desbordes (MSKI); Wendy Lynn Havran (Scripps); and Richard Lifton, Haifan Lin, Diane Krause, and Natalia Ivanova (Yale Uuniversity). Randall Kramer (UCSF) provided the integrin α7 antibody. Bruce Morgan (Harvard) provided the Shh Cre-ER mice. V.G was a Human Frontier Science Program fellow. T.C is a fellow of the New York Stem Cell Foundation and the recipient of an American Association of Cancer Research-Astellas Fellowship for Basic Cancer Research. E.F. is an Investigator of the Howard Hughes Medical Institute. This work was supported in part from a grant from the NIH (E.F.).

References

Alonso L, Okada H, Pasolli A, Wakeham A, You-Ten A, Mak T, Fuchs E. Sgk3 links growth factor signaling to maintenance of progenitor cells in the hair follicle. J Cell Biol 2005;15:559–570. [PubMed: 16103225]

Andl T, Ahn K, Kairo A, Chu EY, Wine-Lee L, Reddy ST, Croft NJ, Cebra-Thomas JA, Metzger D, Chambon P, et al. Epithelial Bmpr1a regulates differentiation and proliferation in postnatal hair follicles and is essential for tooth development. Development 2004;131:2257–2268. [PubMed: 15102710]

Barrandon Y, Green H. Three clonal types of keratinocyte with different capacities for multiplication. Proc Natl Acad Sci USA 1987;84:2302–2306. [PubMed: 2436229]

Blanpain C, Lowry WE, Geoghegan A, Polak L, Fuchs E. Self-renewal, multipotency, and the existence of two cell populations within an epithelial stem cell niche. Cell 2004;118:635–648. [PubMed: 15339667]

Botchkarev VA, Botchkareva NV, Nakamura M, Huber O, Funa K, Lauster R, Paus R, Gilchrest BA. Noggin is required for induction of the hair follicle growth phase in postnatal skin. FASEB J 2001;15:2205–2214. [PubMed: 11641247]

Cotsarelis G, Sun TT, Lavker RM. Label-retaining cells reside in the bulge area of pilosebaceous unit: implications for follicular stem cells, hair cycle, and skin carcinogenesis. Cell 1990;61:1329–1337. [PubMed: 2364430]

Gat U, DasGupta R, Degenstein L, Fuchs E. De Novo hair follicle morphogenesis and hair tumors in mice expressing a truncated beta-catenin in skin. Cell 1998;25:605–614. [PubMed: 9845363]

Guo L, Degenstein L, Fuchs E. Keratinocyte growth factor is required for hair development but not for wound healing. Genes Dev 1996;10:165–175. [PubMed: 8566750]

Hébert JM, Rosenquist T, Götz J, Martin GR. FGF5 as a regulator of the hair growth cycle: evidence from targeted and spontaneous mutations. Cell 1994;78:1017–1025. [PubMed: 7923352]

Horsley V, Aliprantis AO, Polak L, Glimcher LH, Fuchs E. NFATc1 balances quiescence and proliferation of skin stem cells. Cell 2008;132:299–310. [PubMed: 18243104]

Ito M, Kizawa K, Hamada K, Cotsarelis G. Hair follicle stem cells in the lower bulge form the secondary germ, a biochemically distinct but functionally equivalent progenitor cell population, at the termination of catagen. Differentiation 2004;72:548–557. [PubMed: 15617565]

Jaks V, Barker N, Kasper M, van Es JH, Snippert HJ, Clevers H, Toftgard R. Lgr5 marks cycling, yet long-lived, hair follicle stem cells. Nat Genet 2008;40:1291–1299. [PubMed: 18849992]

Kobielak K, Pasolli HA, Alonso L, Polak L, Fuchs E. Defining BMP functions in the hair follicle by conditional ablation of BMP receptor IA. J Cell Biol 2003;163:609–623. [PubMed: 14610062]

Kobielak K, Stokes N, de la Cruz J, Polak L, Fuchs E. Loss of a quiescent niche but not follicle stem cells in the absence of bone morphogenetic protein signaling. Proc Natl Acad Sci USA 2007;104:10063–10068. [PubMed: 17553962]

Levy V, Lindon C, Harfe BD, Morgan BA. Distinct stem cell populations regenerate the follicle and interfollicular epidermis. Dev Cell 2005;9:855–861. [PubMed: 16326396]

Lo Celso C, Prowse D, Watt F. Transient activation of beta-catenin signalling in adult mouse epidermis is sufficient to induce new hair follicles but continuous activation is required to maintain hair follicle tumours. Development 2004;131:1787–1799. [PubMed: 15084463]

Lowry WE, Blanpain C, Nowak JA, Guasch G, Lewis L, Fuchs E. Defining the impact of beta-catenin/Tcf transactivation on epithelial stem cells. Genes Dev 2005;19:1596–1611. [PubMed: 15961525]

Lyle S, Christofidou-Solomidou M, Liu Y, Elder DE, Albelda S, Cotsarelis G. Human hair follicle bulge cells are biochemically distinct and possess an epithelial stem cell phenotype. J Investig Dermatol Symp Proc 1999;4:296–301.

Merrill BJ, Gat U, DasGupta R, Fuchs E. Tcf3 and Lef1 regulate lineage differentiation of multipotent stem cells in skin. Genes Dev 2001;15:1688–1705. [PubMed: 11445543]

Morris RJ, Potten CS. Highly persistent label-retaining cells in the hair follicles of mice and their fate following induction of anagen. J Invest Dermatol 1999;112:470–475. [PubMed: 10201531]

Morris RJ, Liu Y, Marles L, Yang Z, Trempus C, Li S, Lin JS, Sawicki JA, Cotsarelis G. Capturing and profiling adult hair follicle stem cells. Nat Biotechnol 2004;22:411–417. [PubMed: 15024388]

Muller-Rover S, Handjiski B, van der Veen C, Eichmuller S, Foitzik K, McKay IA, Stenn KS, Paus R. A comprehensive guide for the accurate classification of murine hair follicles in distinct hair cycle stages. J Invest Dermatol 2001;117:3–15. [PubMed: 11442744]

Muller-Rover S, Tokura Y, Welker P, Furukawa F, Wakita H, Takigawa M, Paus R. E- and P-cadherin expression during murine hair follicle morphogenesis and cycling. Exp Dermatol 1999;8:237–246. [PubMed: 10439220]

Nguyen H, Rendl M, Fuchs E. Tcf3 governs stem cell features and represses cell fate determination in skin. Cell 2006;127:171–183. [PubMed: 17018284]

Nowak JA, Polak L, Pasolli HA, Fuchs E. Hair follicle stem cells are specified and function in early skin morphogenesis. Cell Stem Cell 2008;3:33–43. [PubMed: 18593557]

Nystul T, Spradling A. An epithelial niche in the *Drosophila* ovary undergoes long-range stem cell replacement. Cell Stem Cell 2007;1:277–285. [PubMed: 18371362]

Oshima H, Rochat A, Kedzia C, Kobayashi K, Barrandon Y. Morphogenesis and renewal of hair follicles from adult multipotent stem cells. Cell 2001;104:233–245. [PubMed: 11207364]

Panteleyev AA, Jahoda CA, Christiano AM. Hair follicle predetermiantion. J Cell Sci 2001;114:3419–3431. [PubMed: 11682602]

Petiot A, Conti FJ, Grose R, Revest JM, Hodivala-Silke KM, Dickson C. A crucial role for Fgrfr2-IIIb signalling in epidermal development and hair follicle patterning. Development 2003;130:3419–3431.

Plikus MV, Mayer JA, de la Cruz D, Baker RE, Maini PK, Maxson R, Chuong CM. Cyclic dermal BMP signalling regulates stem cell activation during hair regeneration. Nature 2008;451:340–344. [PubMed: 18202659]

Rendl M, Lewis L, Fuchs E. Molecular dissection of mesenchymal-epithelial interactions in the hair follicle. PLoS Biol 2005;3:e331.10.1371/journal.pbio.0030331 [PubMed: 16162033]

Rendl M, Polak L, Fuchs E. BMP signaling in dermal papilla cells is required for their hair follicle-inductive properties. Genes Dev 2008;22:543–557. [PubMed: 18281466]

Rhee H, Polak L, Fuchs E. Lhx2 maintains stem cell character in hair follicles. Science 2006;312:1946–1949. [PubMed: 16809539]

Schmidt-Ullrich R, Paus R. Molecular principles of hair follicle induction and morphogenesis. Bioessays 2005;27:247–261. [PubMed: 15714560]

Schofield R. The relationship between the spleen colony-forming cell and the haemopoietic stem cell. Blood Cells 1978;4:7–25. [PubMed: 747780]

Suzuki K, Yamanishi K, Mori O, Kamikawa M, Andersen B, Kato S, Toyoda T, Yamada G. Defective terminal differentiation and hypoplasia of the epidermis in mice lacking the Fgf10 gene. FEBS Lett 2000;481:53–56. [PubMed: 10984614]

Taylor G, Lehrer MS, Jensen PJ, Sun TT, Lavker RM. Involvement of follicular stem cells in forming not only the follicle but also the epidermis. Cell 2000;102:451–461. [PubMed: 10966107]

Tumbar T, Guasch G, Greco V, Blanpain C, Lowry WE, Rendl M, Fuchs E. Defining the epithelial stem cell niche in skin. Science 2004;16:359–363. [PubMed: 14671312]

Van Mater D, Kolligs FT, Dlugosz AA, Fearon ER. Transient activation of beta-catenin signaling in cutaneous keratinocytes is sufficient to trigger the active growth phase of the hair cycle in mice. Genes Dev 2003;15:1219–1224. [PubMed: 12756226]

Vidal VP, Chaboissier MC, Lutzkendorf S, Cotsarelis G, Mill P, Hui CC, Ortonne N, Ortonne JP, Schedl A. Sox9 is essential for outer root sheath differentiation and the formation of the hair stem cell compartment. Curr Biol 2005;15:1340–1351. [PubMed: 16085486]

Waghmare SK, Bansal R, Lee J, Zhang YV, McDermitt DJ, Tumbar T. Quantitative proliferation dynamics and random chromosome segregation of hair follicle stem cells. EMBO J 2008;27:1309–1320. [PubMed: 18401343]

Werner S, Smola H, Liao X, Longaker MT, Krieg T, Hofschneider PH, Williams LT. The function of KGF in morphogenesis of epithelium and reepithelialization of wounds. Science 1994;266:819–822. [PubMed: 7973639]

Zhang Y, Andl T, Yang S, Teta M, Liu F, Seykora J, Tobias J, Piccolo S, Schmidt-Ullrich R, Nagy A, et al. Activation of {beta}-catenin signaling programs embryonic epidermis to hair follicle fate. Development 2008;135:2161–2172. [PubMed: 18480165]

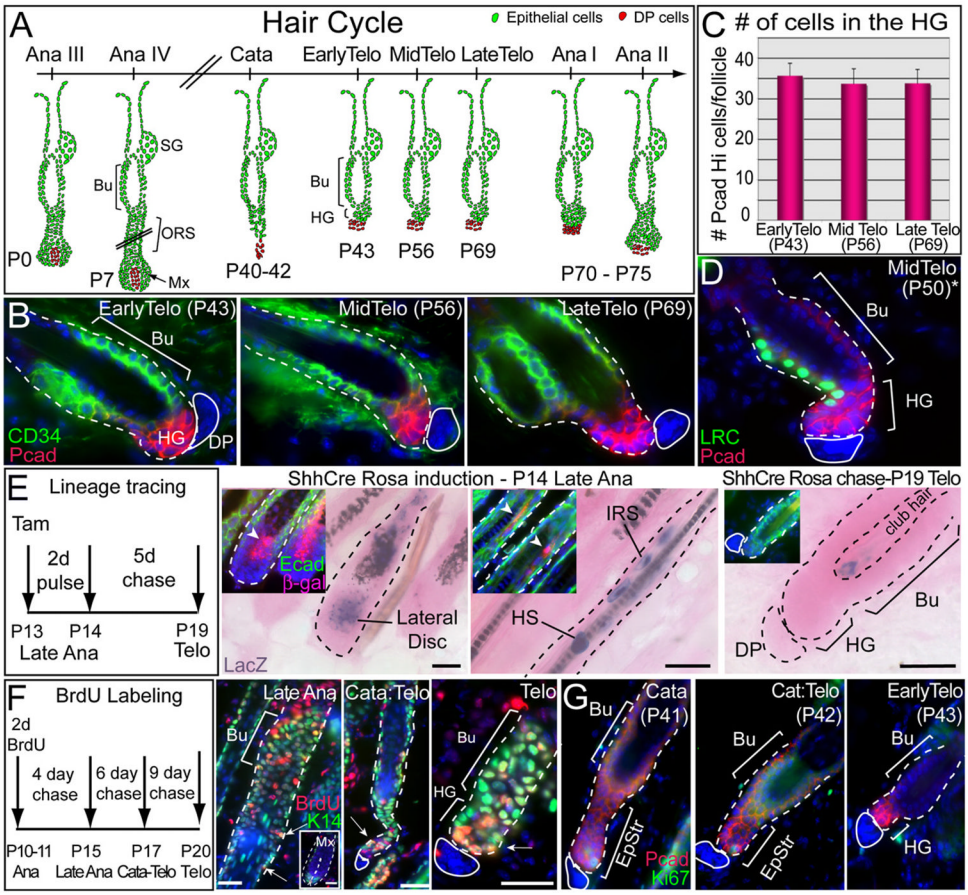

Figure 1. The HG Forms at the Catagen-to-Telogen Transition but Does Not Originate from the Shh-Expressing Lateral Disc

(A) Schematic of the hair cycle. Timing is based upon CD1 mice. Anagen is subdivided into six stages according to Muller-Rover et al. (2001). Hair germs (HGs) emerge at the end of the first catagen and exist as a distinct entity during telogen. Bu, bulge; SG, sebaceous gland; ORS, outer root sheath; Mx, matrix.

(B) HG and bulge are distinguished by immunofluorescence for enrichment of P-cadherin (Pcad, HG) and CD34 (Bu) and by proximity to the dermal papilla (DP), denoted by the solid white line. Note that CD34 marks dermal cells as well as bulge.

(C) HG size is constant during telogen. Confocal Z stack of 100 μm thick sections revealed ~32 cells/HG. Ten representative HFs were scanned at high resolution with 40× objective at the confocal for each time point. In all graphics, data are reported as average ± SD.

(D) Label-retaining cells (LRCs) are present in bulge and HG. Representative section is from H2BGFP pulse chased mouse. *Due to strain difference, mid telogen in *K5Tet^{off}/TRE-H2BGFP* mice is at P50.

(E) Genetic lineage tracing using *ShhCre^{ER}/Rosa-LoxP-Stop-LoxP-LacZ* transgenic mice. Cre was induced with tamoxifen, and mice were analyzed at times shown for β-galactosidase activity (blue) and histology (eosin) (main frames) or Abs to β-gal (red) and Ecadherin (green) (insets). Note β-gal in lateral disc, inner root sheath (IRS), hair shaft (HS), and club hair, but not HG.

(F) BrdU-label-retaining experiments. A 2 day BrdU pulse in anagen was chased for the times indicated and analyzed by immunofluorescence with K14 H2B GFP (green) and BrdU (red) Ab. Note that ORS LRCs (arrow) persist during catagen and can be found in the retracting epithelial strand. At telogen, epithelial LRCs are present in HG (arrow) and bulge.

(G) Nuclear Ki67 immunofluorescence reveals that the bulge (Bu) is largely negative (dormant) during catagen and at telogen. Nuclei are marked blue.

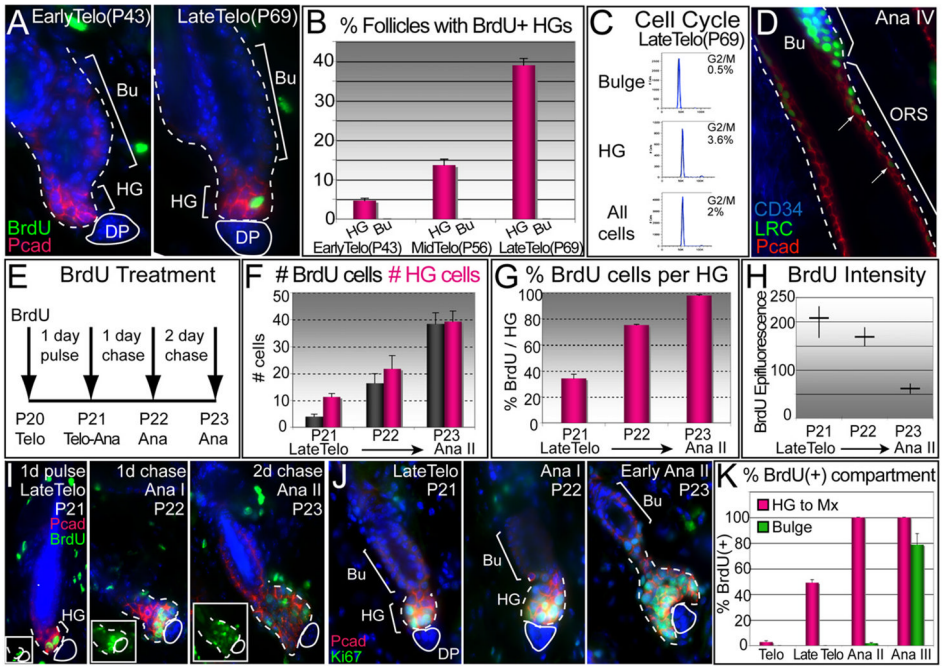

Figure 2. HGs Become Activated Prior to the Bulge and Contribute to the Next Hair Cycle

(A and B) BrdU 1 day pulses were given at early, mid-, and late telogen, followed by analyses. Shown are representative images (A), quantifications compiled from two independent experiments (B). Data are reported as average ± SD.

(C) Cell-cycle profile of purified late telogen populations analyzed by FACS and FlowJo Program.

(D) Representative section from 10 wk *K5Tet*^{off}*/TRE-H2BGFP* mice chased at 4 weeks. During full anagen, LRCs (green) form a trail from the bulge along the ORS (red). Dotted white lines demarcate dermis from HF.

(E–I) Short pulse-chase experiments. Late telogen P20 mice were pulsed with BrdU for 1 day to specifically mark the HG and then chased. Note the increases in BrdU(+) and HG cells per follicle in the transition from telogen to anagen (F and G), while the BrdU intensity decreased (H). Representative pictures of anti-BrdU immunofluoresences are shown in (I).

(J) Ki67 immunostaining to show proliferative cells at the telogen-to-anagen transition.

(K) Short BrdU pulse experiment reveals a two-step activation process: HGs become positive for BrdU by late telogen, while bulge cells remain dormant until the end of anagen II. Nuclei are marked with DAPI (blue).

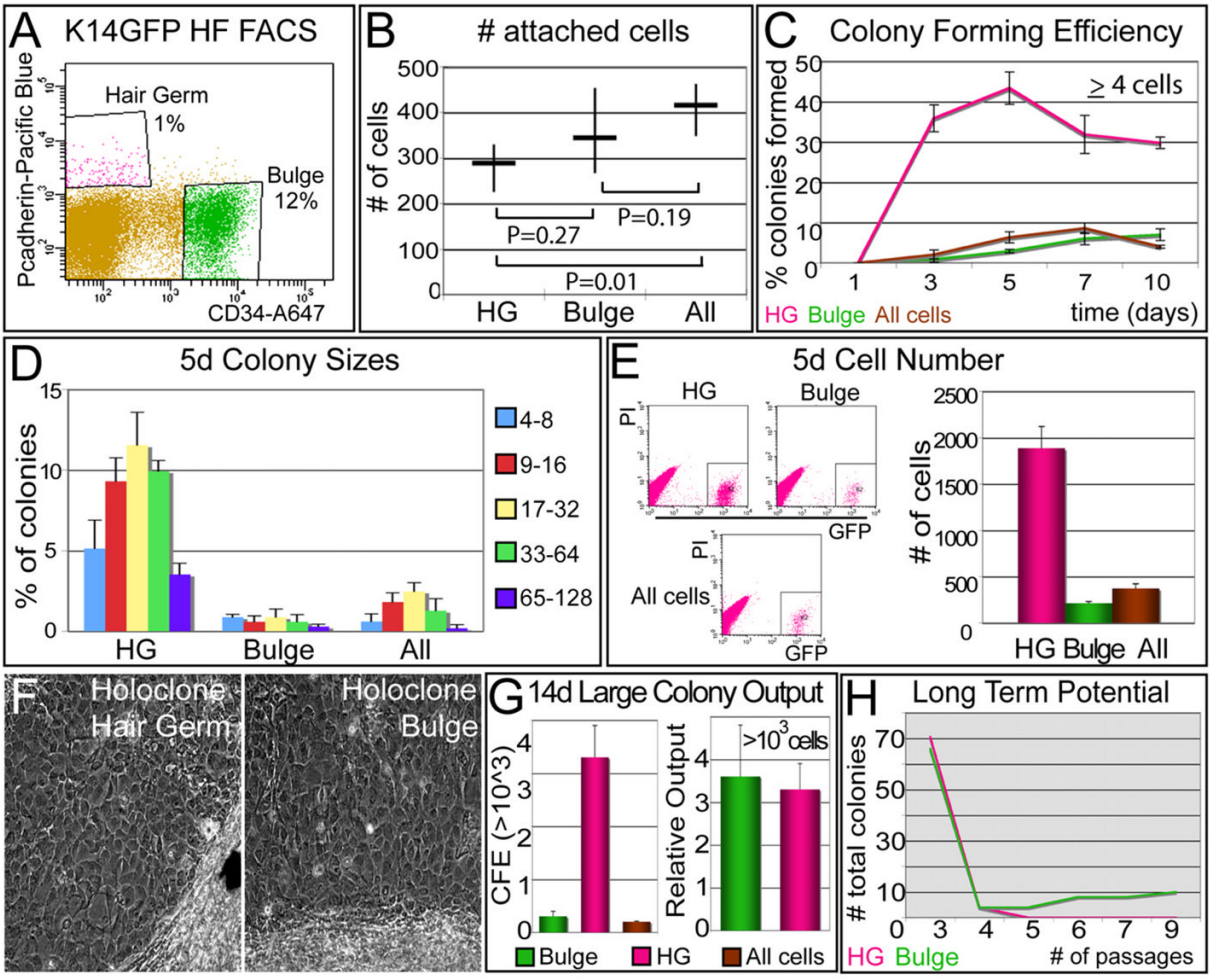

Figure 3. HG Cells Form Large Colonies Faster than Bulge Cells, but Their Long Term Potential is Poorer In Vitro

(A) FACS profile for isolating HG and bulge cells from P69 *K14H2BGFP* female CD1 mice. The "All" fraction is all GFP(+).

(B) 10^3 cells of each population were plated in quadruplicate onto 12-well plates, and 12 hr later, the numbers of attached cells were quantified. The same experiment was performed in parallel in 6-well plates with no significant differences observed.

(C) Colony forming efficiency. We measured the percent (%) of attached cells that proliferated to reach a size of ≥4 cells (a colony) (Barrandon and Green, 1987). Graphs show average percentage ± SD. Note that HG cells formed colonies efficiently, but by 10 days, they began to diminish.

(D and E) Colony sizes and total cell number after 5 days in vitro. Experiments were performed in quadruplicate.

(F and G) Large colonies formed after 14 days in vitro. FACS-purified HG, bulge, and all GFP(+) cells were plated and monitored over 2 weeks. (F) Morphological appearance of a large (>20 mm^2; 10^3 cells) colony formed from individual HG or bulge cells. Note tightly packed, relatively undifferentiated cells within HG and bulge colonies. (G) Left graph depicts the percent (%) large colonies formed relative to an equal number of cells plated. Right graph depicts total number of large colonies per population. Since bulge contains ~12× more cells than HG, their total output of large colonies is comparable.

(H) Long-term potential. Individual large clones were dissociated and serially passaged in culture. Note that most HG clones did not survive past passage 3, even when transferred as a whole to enhance the probability of holoclone detection.

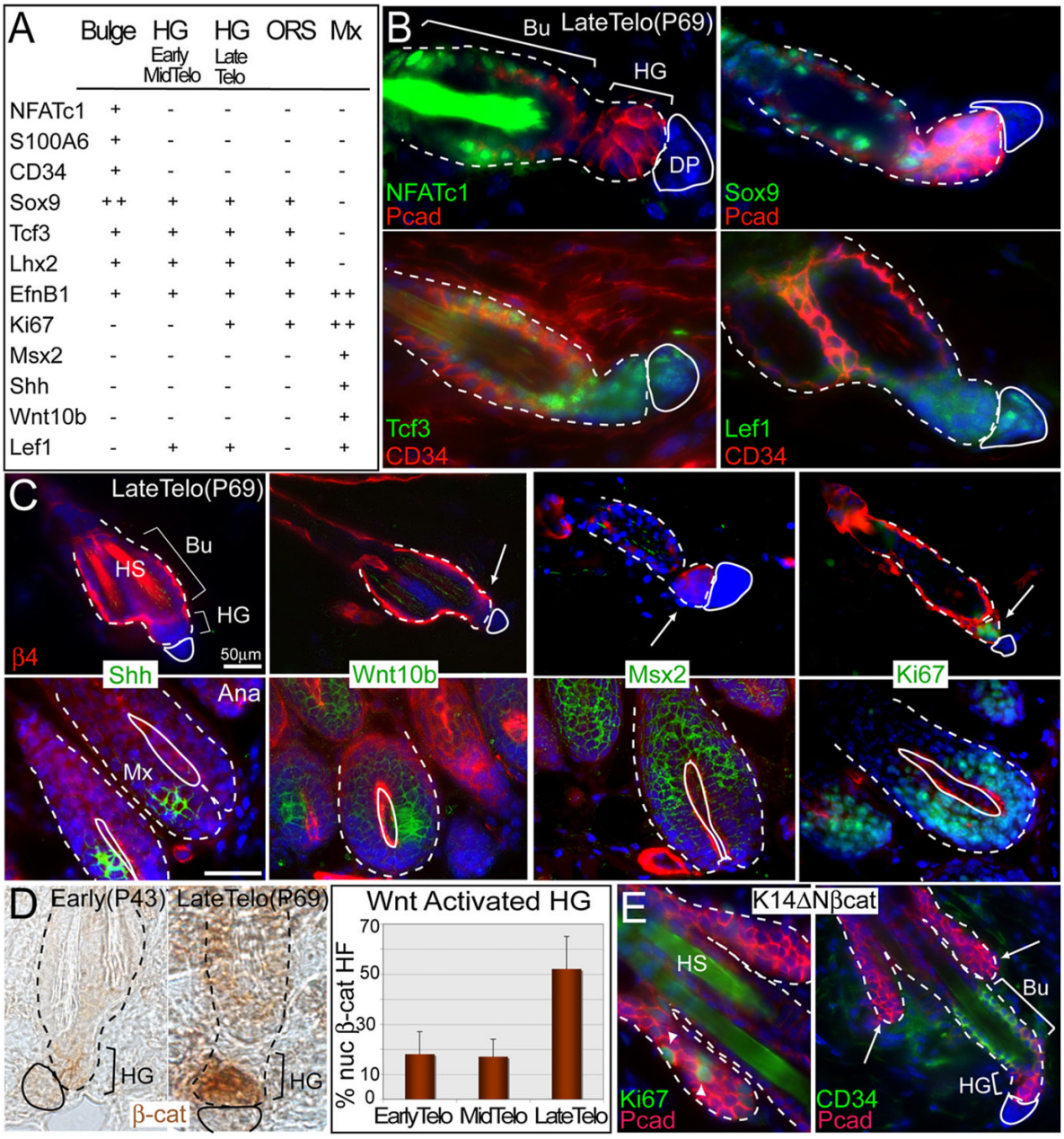

Figure 4. The HG Is Molecularly Distinct from Bulge, ORS, and Matrix and Displays Elevated Nuclear β-Catenin When Activated

(A) Table summarizing HG expression patterns of classical HF markers.

(B and C) Confirmation of HG expression patterns by in situ hybridizations *(Shh*, *Wnt10b*, and *Msx2*) or immunofluorescence (rest). Arrows denote HGs. In (C), anti-β4 integrin (red) marks bulge and HG (hair shafts, HS, autofluorescence). White solid line delineates DP; dotted line denotes dermo-epithelial boundary.

(D) Immunohistochemistry shows nuclear localization of β-catenin only in late telogen HGs (quantification reported as average ± SD).

(E) Immunofluorescence of backskin sections of *K14ΔNβcat* transgenic mice expressing constitutively stabilized β-catenin. Note that ectopic de novo HFs (arrows) are proliferative

(arrowheads point to Ki67+ nuclei) and enriched for HG marker P-cadherin (in red), but not bulge marker CD34 (in green right panel). Nuclei are marked with DAPI (blue).

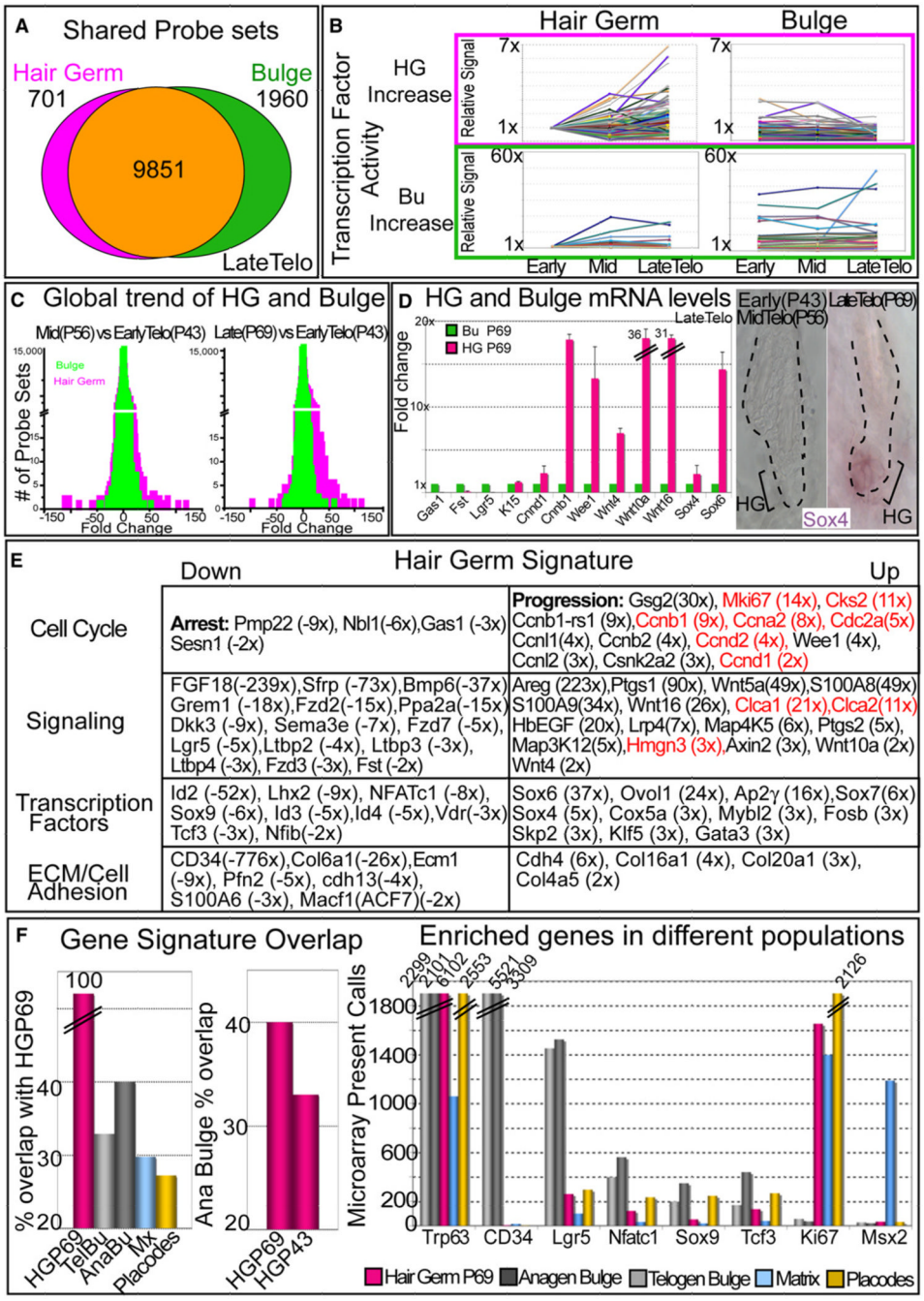

Figure 5. Prior to a New Hair Cycle, HGs Are Transcriptionally More Active than the Bulge

HG and bulge cells were FACS purified from P43, P56, and P69 HFs, and their mRNAs were subjected to microarray analyses.

(A) Venn diagram reveals degree of similarity between P69 HG and bulge based on absolute present calls. 701 probe sets are uniquely present in the HG and absent in the bulge; 1960 probe sets are unique to the bulge.

(B) Genes in DAVID-scored enriched categories (see the Supplemental Experimental Procedures) are more dynamically expressed during telogen in the HG versus bulge.

(C) Global changes in HG versus bulge expression profiles between any two time points in telogen. Note that differences are more pronounced for HG than bulge.

(D and E) Array comparisons between HG and bulge define a molecular signature that distinguishes the two populations at each of the three time points throughout telogen. Shown are data for P69, where the differences are most conspicuous. Real-time PCR or in situ hybridization in (D) validates key genes of the P69 molecular signatures, summarized in (E). Data are reported as average ± SD. Genes highlighted in red are part of a shortlist whose expression is upregulated in anagen versus telogen bulge cells when the levels of stabilized β-catenin are elevated (Lowry et al., 2005). Fold differences are indicated in parentheses. (F) Comparisons between the late telogen HG array signals and those of the telogen bulge (TelBu) (Lowry et al., 2005), anagen bulge (AnaBu) (Lowry et al., 2005), matrix (Mx) (Rendl et al., 2005), and embryonic hair placode/primary hair germ (Rhee et al., 2006). Key gene array levels from each population are plotted in histograms at right. These comparisons underscore the uniqueness of the HG.

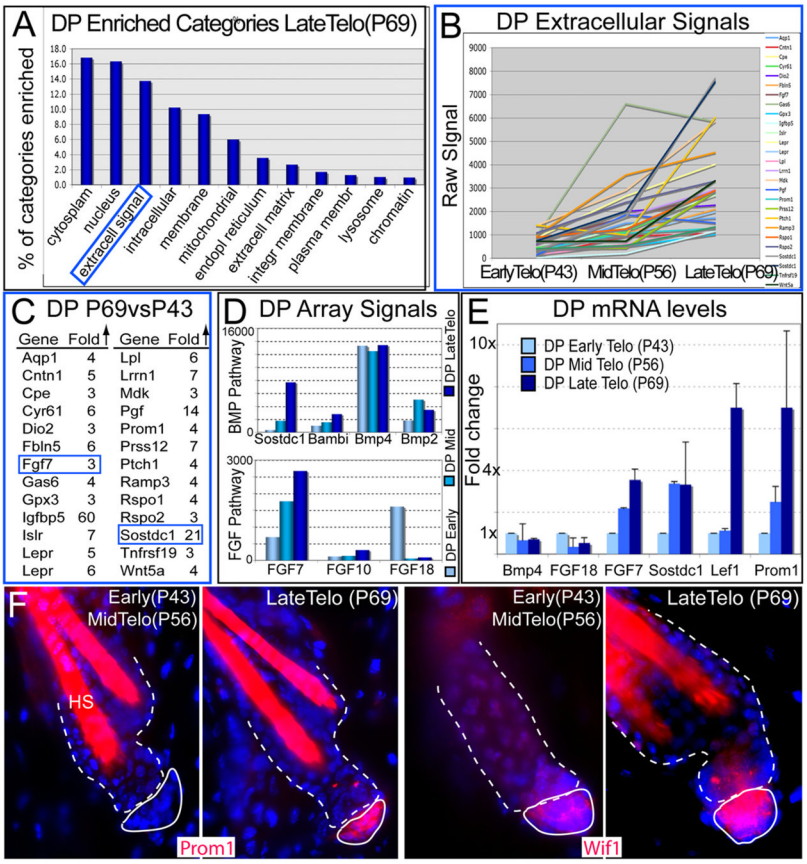

Figure 6. DP Cells Are Also Transcriptionally Active during the Quiescent Phase

HG, bulge and DP were simultaneously FACS purified from P43, P56 and P69 HFs and then subjected to microarray analyses.

(A) Gene Ontology comparisons reveal several gene categories enriched progressively as the DP transitions through telogen. Note the extracellular signaling molecules were among the most enriched of the specialized categories.

(B and C) Trend and list of DP genes belonging to the extracellular signaling category and that are upregulated (>3×) with signal values ≥1000 at late versus early telogen.

(D) Microarray DP signal values of BMP and FGF pathway members, which displayed particularly prominent temporal differences across telogen. FGF7 and BMP inhibitors Sostdc1 and Bambi progressively increased in expression during telogen, in comparison to BMPs 2 and 4.

(E) Real-time PCR of mRNAs from purified DP confirms the trends observed from the microarrays. Data are reported as average ± SD.

(F) Immunofluorescence of Prom1 and Wif1 confirm their differential expression patterns in the DP during telogen. DAPI in blue; hair shafts (HS) are autofluorescent.

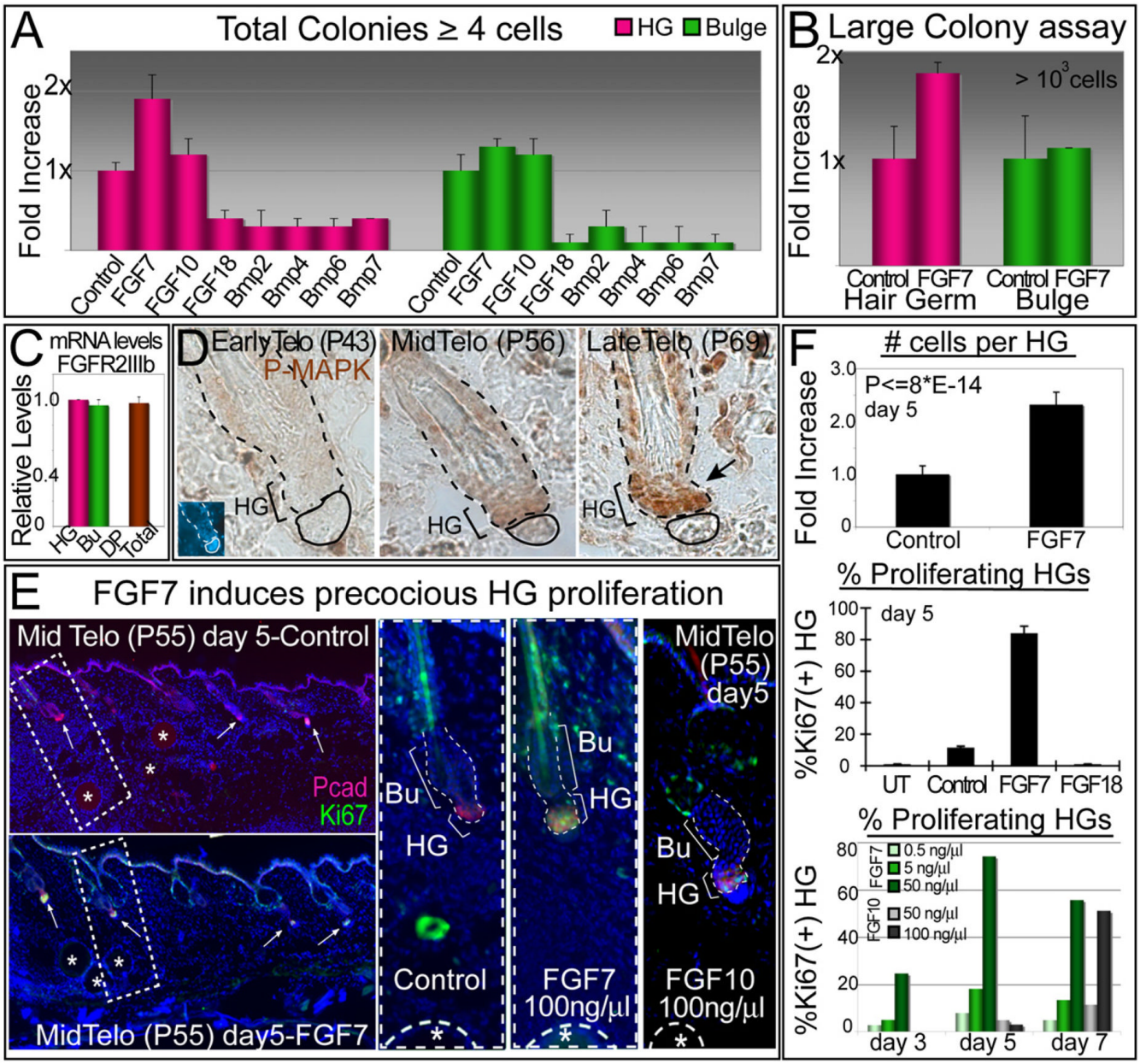

Figure 7. FGF7 Stands Out As a DP Effector of HG Cell Growth that Increases in Expression during Telogen

(A) In culture, FGF7 increases the total number of colonies made by HG cells. Bulge cells are affected to a lesser extent. Same assay as in Figure 3D over a course of 5 days was used to assess the effect of the various factors.

(B) FGF7 displays a similar positive effect on the formation of large colonies from HG cells.

(C) Real-time PCR of FGFR2 *exon IIIb*, specific for the FGF7/FGF10 receptor. Note presence in HG and bulge, but not DP, supportive of paracrine action.

(D) Abs against phosphorylated (active) MAPK reveal signs of growth factor signaling during late telogen, concomitant with the elevation in *FGF7* expression

(E and F) FGF7 treatment in vivo precociously activates HG cells and induces them to proliferate. P50 CD1 mice whose HFs were in early telogen were injected with beads soaked in factors as indicated. Experiments were done ≥2 for all factors, and ~50 HFs per mouse

were analyzed. After 5 days of treatment, nearly 100% of HFs were Ki67(+) and displayed enhanced numbers of cells within the HG. By contrast, HFs that were either untreated (UT) or treated with BSA (Control) or FGF18 remained dormant during telogen (middle histogram). The effects of FGF7 and FGF10 were similar with FGF7 showing more potent effects (lower histogram). In all graphics, data are reported as average ± SD.